Disease Modifying Effects of N-butyryl Glucosamine in a Streptococcal Cell Wall Induced Arthritis Model in Rats

SUSANNE X. WANG, ANNIE CHERIAN, MIRCEA DUMITRIU, MARC D. GRYNPAS, JOHN CARRAN, DAN WAINMAN, and TASSOS ANASTASSIADES

ABSTRACT. ***Objective.*** To evaluate the effect of different doses of N-butyryl glucosamine (GlcNBu) on joint preservation and subchondral bone density and quality in a streptococcal cell wall (SCW) induced arthritis model in Lewis rats.

Methods. Chronic arthritis was induced in 36 female Lewis rats by a single intraperitoneal injection of SCW antigen. The 4 groups studied were: (1) no arthritis, no drug treatment; (2) arthritis, no drug treatment; (3) arthritis, oral GlcNBu 20 mg/kg/day; and (4) arthritis, oral GlcNBu 200 mg/kg/day. Inflammation (ankle swelling) was quantified throughout the clinical course; bone mineral density (BMD) was measured by dual-energy x-ray absorptiometry on dissected distal femurs and proximal tibiae, in user defined regions of interest. Qualitative and quantitative 3-D bone architecture changes were determined using microcomputerized tomography on the left tibiae. Subchondral plate thickness and trabecular bone connectivity were studied on the proximal tibia epiphyses from the central coronal sections of each scanned tibia.

Results. GlcNBu inhibited inflammatory ankle swelling at both 20 and 200 mg/kg/day, the latter being statistically significant, with an average reduction of 33%. GlcNBu preserved or enhanced BMD and bone connectivity and prevented further bone loss at both the high and the low dose. Comparisons of the isosurfaces and the architectural measures in the different groups showed that GlcNBu effectively protected the joint surfaces from further erosion in this model of chronic inflammatory arthritis. For some of the bone measurements, increasing doses of GlcNBu showed increasing protective effects, while for other measurements, effects were maximal at the lower dose.

Conclusion. These data indicate that GlcNBu provides antiinflammatory and antierosive effects by preserving BMD, joint integrity, and bone architecture in involved joints of the SCW model. (First Release Feb 15 2007; J Rheumatol 2007;34:712–20)

Key Indexing Terms:
N-BUTYRYL GLUCOSAMINE STREPTOCOCCAL ARTHRITIS RATS

Rheumatoid arthritis (RA) and osteoarthritis (OA) both demonstrate prominent bone remodeling, although the histopathology of the subchondral bone, its relation to damaged cartilage, and the rates of remodeling are considerably different[1-3]. A number of cytokines, biochemical markers, and gene expression alterations that reflect cartilage or bone turnover and disease progression have been reported, some of which may be seen very early[4-6].

In RA, damage to articular cartilage begins at the cartilage–pannus interface, but there are also progressive erosions occurring into the subchondral bone. The pattern of bone damage in the joint includes focal erosions and juxtaarticular osteopenia. The effect of RA on bone, however, is also observed systemically in the axial and appendicular skeleton, with reductions in bone mineral density (BMD) causing osteoporosis and, as a consequence, increased risk of fracture[7,8]. Many patients with RA have radiographic evidence of substantial joint damage within the first 2 years of disease[9], and even in the first few months, evidence of bone erosion may be seen with magnetic resonance imaging[10,11]. Further, bone loss is a typical pathological feature of RA. The skeletal target most exposed to inflammatory damage is the subchondral bone adjacent to inflamed synovial tissue. Early after disease onset, this particular area faces rapid destruction, which results in the typical radiologic signs of RA, manifested as

From the Department of Laboratory Medicine and Pathobiology, University of Toronto, and Samuel Lunenfeld Research Institute, Mount Sinai Hospital, Toronto; Department of Medicine, Arthritis Center; and Departments of Biochemistry and Chemistry, Queen's University, Kingston, Ontario, Canada.

Supported by CIHR Proof of Principle Grant 20020PPP and Strategic NSERC Grant STPG 246039-01 (both to T. Anastassiades).

S.X. Wang, MD; A. Cherian, BSc; M. Dumitriu, PhD; M.D. Grynpas, PhD, Department of Laboratory Medicine and Pathobiology, University of Toronto, and Samuel Lunenfeld Research Institute, Mount Sinai Hospital; J. Carran, PhD, Department of Medicine, Arthritis Center and Department of Chemistry; D. Wainman, BT, Department of Medicine, Arthritis Center; T. Anastassiades, MD, PhD, FRCP, Department of Medicine, Arthritis Center, and Department of Biochemistry, Queen's University.

Address reprint requests to Dr. T. Anastassiades, Division of Rheumatology, Department of Medicine, Room 2050, Etherington Hall, Queen's University, Kingston, ON, K7L 4B4. E-mail: anastass@post.queensu.ca

Accepted for publication December 12, 2006.

local bone erosion and periarticular demineralization[12]. However, erosive changes also occur more centrally that are related to inflammatory changes in the subchondral marrow spaces, and remodeling of the subchondral bone is a feature of disease progression[13].

Destruction of bone has become a synonym for irreversible tissue damage and poor functional outcome in patients with RA[14-16], and its prevention underlies an important therapeutic principle of antirheumatic drug therapy. The gold standard for evaluating bone destruction in patients with RA is the visual scoring of radiographs of the hands for joint erosions and narrowing[17,18]. The scores obtained correlate highly with the quantitative measurement of metacarpal cortical width, which declines with RA progression due to accelerated bone loss at the endosteal surface[19]. Computerized tomography (CT) has been shown to be more sensitive than radiography in detecting bone erosions in patients with RA, due to its 3-dimensional (3-D) perspective[20]. Micro-CT has proven to be a powerful technique to analyze bone structure and density in small animals.

Evaluation of current therapies for RA by metaanalysis of randomized clinical trials (RCT) demonstrates significant toxicity with currently used antirheumatic drugs, although risk/benefit ratios appear to be improving compared to previous treatments[21]. Efficacious therapies with very low toxicity are not available for RA. In OA, glucosamine (GlcN) or glucosamine sulfate (GlcN.S), a non-covalently bound sulfate salt of GlcN, are considered to constitute very low toxicity therapies. However, metaanalysis of available RCT[22], as well as clinical studies where GlcN was withdrawn[23], renders the question of efficacy of these compounds controversial for OA. The efficacy of GlcN compounds has not been evaluated in RA.

A different and novel approach to drug development for diseases of joints consists of utilizing an abundant, nontoxic, naturally occurring parent carbohydrate, such as GlcN, and chemically modifying it to yield products that are similar, but not identical, to those that occur in nature. GlcN occurs in matrix and cellular glycoconjugates largely in the N-acetylated form, N-acetyl GlcN (GlcNAc). Chemical N-acylation of glucosamine leads to a class of compounds that exhibit biological activity that is markedly different from their parent GlcN[24]. Among these GlcNAcyl, which were initially developed as chondroprotective agents, N-butyryl glucosamine, N-(2,4,5-trihydroxy-6-hydroxymethyl-tetrahydro-pyran-3-yl)-butyramide, (GlcNBu) is the most studied and preferred compound of the synthetic GlcNAcyl. This is because of its chemical properties, lack of toxicity in animal, cell culture and genotoxicity studies, and the biological activity profile[25]. Compared to GlcN, which was found to have suppressive effects on bovine chondrocyte proliferation and proteoglycan (PG) synthesis, GlcNBu demonstrated stimulatory effects. The differences between GlcN and the GlcNAcyl were marked under high concentrations and were more prominent under anchorage-dependent compared to anchorage-independent culture conditions. Also, GlcNBu upregulated a number of genes in human OA chondrocytes, compared to GlcN[25]. These effects were seen in both the presence and absence of the cartilage and bone regulatory peptide transforming growth factor-ß (TGF-ß), which is related to the bone morphogenetic protein supergene family. In addition, GlcNBu increased type II collagen expression by rat chondrocytes[26]. GlcNBu and similar GlcNAcyl are good substrates for glycosyltransferases from bone and cartilage cells[27], although their mechanism of action for the biological effects has not been established. Recently, a high performance liquid chromatography method for quantification of GlcNBu in rat plasma has been developed[28]. The method is linear over the range of 0.2–200 mg/ml, and was applied to oral administration of GlcNBu in the rat.

For preclinical evaluation of GlcNBu, a number of animal models have been considered. Some OA models depend on altering joint biomechanics by disrupting the anterior cruciate ligament of the knee, as in the dog or rabbit[29]. Such models are time consuming and relatively expensive, partially because of the number of animals required to overcome variability. The rabbit model[29] has provided preliminary results of interest with oral feeding of GlcNBu that are being analyzed histologically. However, inflammatory stimuli can provide rapid remodeling of bone and cartilage in the joint[1]. The Lewis rat (LEW/N) model has been well studied and is particularly susceptible to induction of arthritis by a single intraperitoneal (IP) injection of streptococcal cell wall (SCW)[30]. In this model, there is an immediate onset of acute arthritis affecting primarily hind leg distal joints, followed (2–3 wks later) by a secondary chronic arthritis, where severe destruction and remodeling of the initially affected joint occurs. The arthritis can be reversed by an injection of anti-TGF-ß antibody[31] and attenuated by splenectomy[32]. Dual-energy x-ray absorptiometry (DEXA) for the assessment of bone density and 3-D CT[33,34] had not been previously applied to the study of drug effects on the bone and cartilage changes in this model.

Our purpose was to determine the effects of orally administered GlcNBu on the inflammation, BMD, and subchondral bone quality measurements in a SCW model in the rat. Micro-CT was employed to quantify the cancellous bone architectural and connectivity changes in rat tibiae.

MATERIALS AND METHODS

Animal model and experimental design. The animal protocol was approved by the Queen's University Animal Care Committee. There was active supervision of the arthritis model by a veterinarian from that service, with respect to ethical treatment of the animals. Forty-two inbred female Lewis rats weighing at least 150 g were purchased from Charles River Laboratories, through Queen's University, and acclimated for at least 1 week prior to use. The rats were housed in filter-capped polycarbonate cages and maintained under constant environmental conditions (average 22°C, humidity 50%). Rats were kept on a 12 h/12 h light–dark cycle and had unrestricted access to purified bottled drinking water and standard chow.

Chronic arthritis was induced in 36 female Lewis rats by a single IP injec-

tion of SCW fragments (15 μg/g) as described[30]. Purified peptidoglycan-polysaccharide polymers (PG-PS 10S, Lee Laboratories, Grayson, GA, USA) were presonicated for 10–20 s prior to injection. The rats were divided into 4 groups according to the induction of disease and supplementation of GlcNBu. The GlcNBu or glucose (for controls with arthritis) were administered in a small amount of peanut butter once a day and was readily ingested by the rats. The 4 groups were (1) control: no arthritis, no treatment, n = 6; (2) SCW induced arthritis, no drug treatment (oral glucose 200 mg/kg/day), n = 12; (3) SCW induced arthritis, low-dose oral GlcNBu-treated (20 mg/kg/day), n = 12; and (4) SCW induced arthritis, high-dose oral GlcNBu-treated (200 mg/kg/day), n = 12.

Inflammation of the ankles was quantified on multiple days by measuring the ankle diameter using a standard caliper method from disease onset to Day 28 after initiation of arthritis. Three measurements were done on each ankle, for each timepoint, to an accuracy of 0.1 mm, and averaged. Animal weights were also monitored daily. At the end of 4 weeks, the animals were sacrificed and both left and right femora were dissected and fixed in 10% neutral buffered formalin for BMD and micro-CT analysis.

BMD measurement. All the dissected femora and tibiae were scanned with DEXA using the PIXImus^{TM} densitometer (GE Lunar Corp., Madison, WI, USA). After calibration with an aluminum/lucite phantom (Lunar Corp./GE), the excised bones were placed on a polystyrene tray to mimic soft tissues for scanning. The PIXImus automatically calculated the areal BMD (aBMD) from the bone mineral content (BMC) and the measured region of interest (ROI)[33]. The BMD (aBMD, g/cm^2) and BMC (g) were measured at the distal femur and proximal tibia using a user-defined ROI.

Micro-CT imaging protocol. The fixed left tibiae were scanned with a micro-CT scanner (Explore Locus SP micro CT scanner; GE Healthcare, London, ON, Canada). The Explore CT acquisition software from General Electric Medical Systems was used to set the scan at 15-μm isotropic voxel size, with 499 projections, and a total scanning time of 70 min. Each tibia was placed in a water-filled specimen tube in a firm position such that the main axis was kept as parallel as possible to the Z-axis of the micro-CT image coordinate system. This minimized any beam-hardening effects, since the radiographic beam crossed a minimal volume of bone tissue. The scan was corrected following image acquisition using data acquired from an empty scan in which bright and dark images were gathered. Correction accounted for variations in temperature and attenuation of the radiographs[34]. The reconstructed tibia images were analyzed with MicroView 2.0 software (GE Healthcare) in 2 and 3 dimensions.

Three-dimensional trabecular bone analysis. Quantitative 3-D bone analyses were conducted with 3 selected ROI using MicroView 2.0 software. Two of the ROI were rectangular with the same dimensions (1.65 mm × 1.65 mm × 0.55 mm) and positioned in the middle of either lateral or medial epiphysis to measure the 3-D microarchitecture of the epiphyseal trabeculae (Figure 1A, 1B). The third ROI (Figure 1C), a cylinder 2 mm in diameter and 1 mm in thickness, was placed 1 mm below the growth plate in the middle of metaphysis to measure the 3-D microarchitecture of the metaphyseal trabeculae.

The micro-CT images were analyzed for bone volume fraction (BVF), reported as percentage of total bone volume, volumetric BMD in mg/ml, average trabecular bone thickness (Tb.Th) and trabecular separation (Tb.Sp) in μm, and trabecular number (Tb.N) per mm^2 of bone surface. The tissue volume (3-D-TV, mm^3) and trabecular bone volume (3-D-BV, mm^3) were measured directly, and the fractional trabecular bone volume (3-D-BV/TV, %) was calculated[35].

The connectivity of the trabecular bone was measured on 2-D skeletonized binary images obtained from a central coronal proximal section from the 3-D micro-CT tibia reconstruction. We used an in-house program based on the techniques described by Parisien, *et al* to define the connectivity measures[36]. The connectivity measures obtained in the analysis include: number of multiple points (mm^{-2}), number of endpoints (mm^{-2}), lengths of node-node struts (mm/mm^2), lengths of free-free struts (mm/mm^2), and total strut length (mm/mm^2). Figure 2A illustrates the area of cancellous bone analyzed by strut analysis and Figure 2B defines strut connectivity measure.

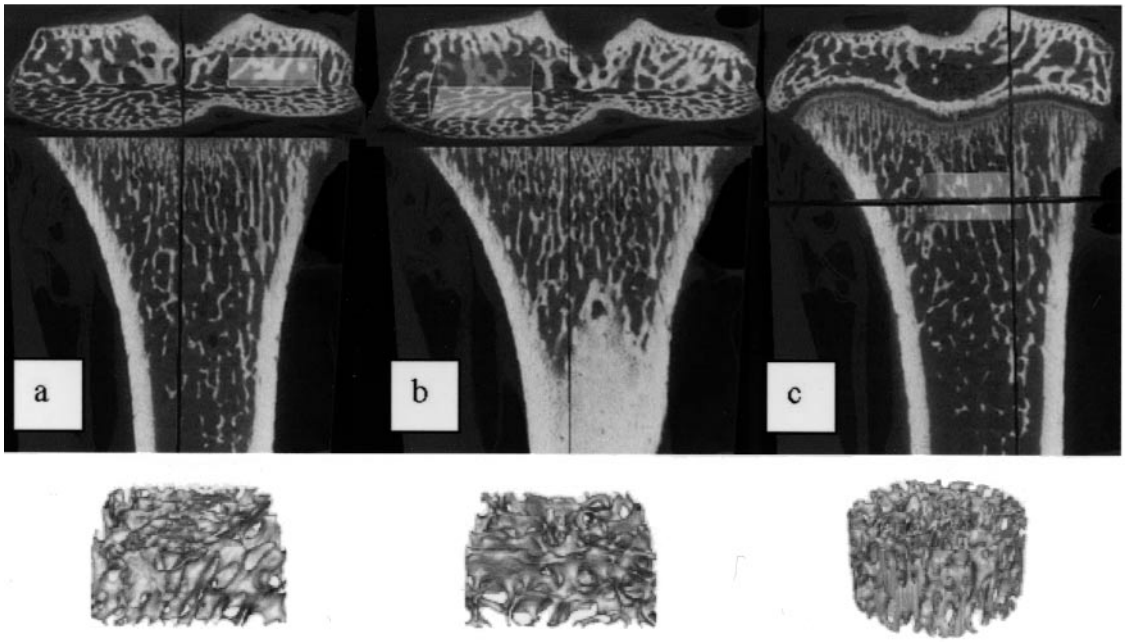

Figure 1. Locations of the regions of interest (ROI) analyzed using the bone analysis application of MicroView. Regions highlighted in A and B are located in the central region of the medial and lateral proximal epiphysis, respectively (mirrored positions). The cylindrical ROI in C was placed 1 mm below the lowest point of growth plate in the central region of the metaphysis. Images in the lower panels are trabecular bone segments analyzed from the ROI indicated above.

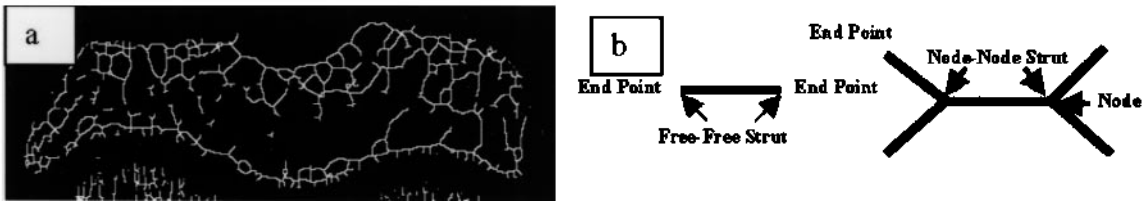

Figure 2. A. The area of cancellous bone analyzed by strut analysis. B. Strut and connectivity measures.

Subchondral plate thickness. A coronal section of the central proximal tibia was obtained from each 3-D reconstructed tibia image. Subchondral plate thickness (SCP.Th, mm) was measured on the central coronal section of the 2-D micro-CT proximal tibia images using individual point-to-point distance measures. The thickness was calculated by averaging 12 measurements per tibia. All measurements were made in a standardized viewing area by a single observer who was blinded to the experiment.

3-D isosurface. A 3-D surface model of each proximal tibia was reconstructed from the CT images by isosurface extraction using the volume-rendering function in MicroView to qualitatively examine the erosive damage in the bone surface. Since the bone destruction was mainly observed in the subchondral bone region adjacent to the inflamed synovial tissue, the proximal surface of the tibiae was used in the analysis.

Statistical analysis. All data were analyzed with SPSS 11.0 for Windows (SPSS Inc., Chicago, IL, USA). One-way analysis of variance with Fisher's least-significant difference post-hoc test was used to compare means. Significance was considered $p < 0.05$. All data are presented as mean ± standard error (SE).

RESULTS

Effects of GlcNBu treatment on the SCW induced inflammation. All the groups increased in weight equally over the 4 week experiment period (data not shown). Ankle size measurements showed that all the animals receiving the IP SCW injection entered the acute phase immediately (Figure 3). Between Days 6 and 12, the acute inflammatory response tended to subside. Approximately 80% of animals in each group entered the chronic phase, at about 2 weeks, partially accounting for the larger SE in the ankle size measurements between Days 14 and 26 (Figure 3). Orally administered GlcNBu at 200 mg/kg/day significantly decreased the swelling compared to the group without treatment (top and middle lines, respectively, in Figure 3). Low-dose GlcNBu treatment (20 mg/kg/day) generated an intermediate response, with a decline in ankle size measurements, which did not reach statistical significance (data not shown).

Decreased BMD and BVF in arthritic bone and reversal by GlcNBu DEXA-measured BMD. A significant decrease ($p < 0.01$) in BMD was seen in both the femora and tibiae of the SCW induced arthritic rats without drug treatment (Figure 4A) compared to the control group. Treatment with GlcNBu

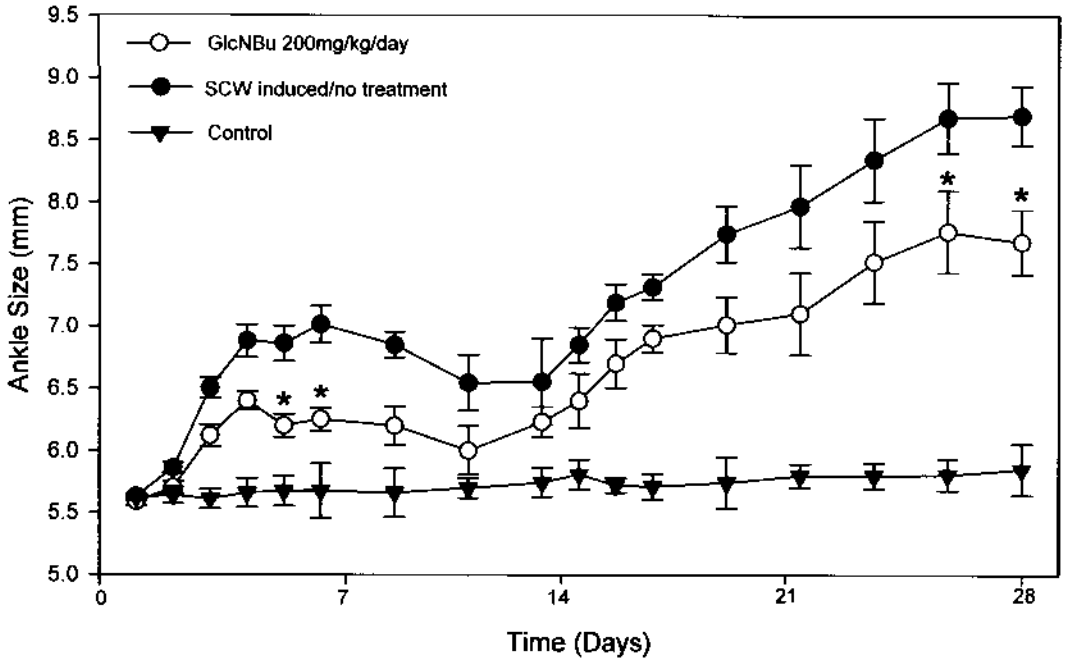

Figure 3. Inhibition of inflammatory ankle swelling in rats with SCW induced adjuvant arthritis by GlcNBu. The no-treatment SCW arthritis group demonstrated continuous joint swelling in comparison to the control animals with no arthritis, throughout the observation period (top and bottom lines, respectively). High-dose GlcNBu at 200 mg/kg/day decreased the swelling significantly compared to the no-treatment SCW arthritis group (*$p < 0.05$). For GlcNBu 20 mg/kg/day (data not shown): Day 5, $p < 0.046$; Day 6, $p < 0.015$.

preserved BMD in the rat tibiae and femora with SCW induced arthritis, and the protective effect occurred in a dose-dependent manner (Figure 4A). With 20 mg/kg/day GlcNBu treatment, the tibia BMD was significantly increased ($p < 0.05$) compared to the SCW induced group. Further, 200 mg/kg/day GlcNBu treatment not only increased BMD in the tibia ($p < 0.05$) but also showed a trend towards a higher BMD in the femur ($p = 0.06$) versus the SCW induced group. Finally, there were no statistical differences between the 200 mg GlcNBu-treatment group and normal controls in both tibia and femur.

Bone volume fraction. BVF measurements using micro-CT presented results similar to the BMD measurements. Figure 4B presents the dose-dependent BVF changes after GlcNBu treatment in 3 different regions — metaphyseal, medial, and lateral epiphyseal. SCW injection caused significantly decreased BVF compared to controls in all 3 compared regions. Treatment with GlcNBu 20 mg/kg/day significantly increased ($p < 0.01$) the tibia metaphyseal BVF compared to the SCW induced group, while a trend towards higher BVF was observed in the epiphyseal lateral region ($0.05 < p < 0.1$). Moreover, 200 mg/kg/day GlcNBu treatment significantly increased BVF in the metaphyseal and epiphyseal lateral regions, while a trend towards higher BVF was observed in the epiphyseal medial region compared to the SCW group.

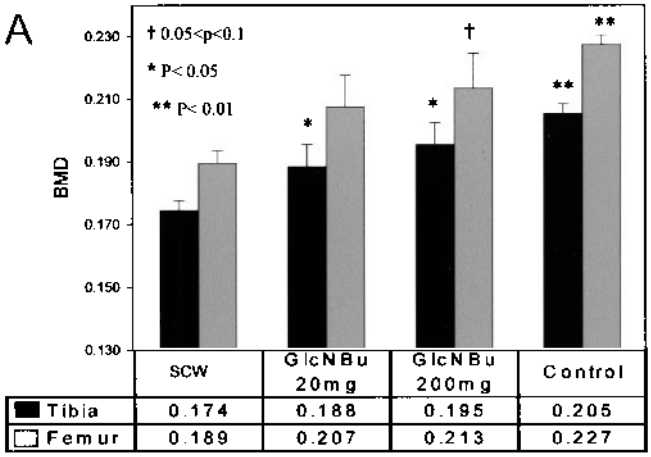

Microarchitecture changes of the trabecular bone. The trabecular BVF, trabecular number, and trabecular thickness were significantly decreased, while the trabecular separation was significantly increased, in the arthritic subchondral bone compared to the controls (Table 1). These changes indicate significant bone loss and inferior bone architecture in the SCW induced arthritis. However, GlcNBu administration strongly suppressed these changes in SCW induced rats. Several measures in the 3 analyzed regions with 20 mg/kg/day GlcNBu treatment were significantly improved from the arthritic change (Table 1). Additionally, the majority of measures were improved with 200 mg/kg/day GlcNBu treatment. These results suggest a dose-dependent effect of GlcNBu on SCW induced arthritic bone changes.

Cancellous bone connectivity. SCW induced arthritis showed significantly less connected cancellous bone compared to controls at all tested sites (Table 2). Although 20 mg/kg/day GlcNBu treatment did not significantly affect bone connectivity, the 200 mg/kg/day GlcNBu treatment increased node-node struts and total strut length in some analyzed sites compared to untreated SCW induced arthritis group (Table 2). This suggests a positive effect of GlcNBu on subchondral bone connectivity.

Subchondral bone plate thickness. Subchondral plate measurements reveal a significant difference in subchondral plate thickness between the SCW induced rats and the controls (Figure 5). A much thinner subchondral plate in the SCW

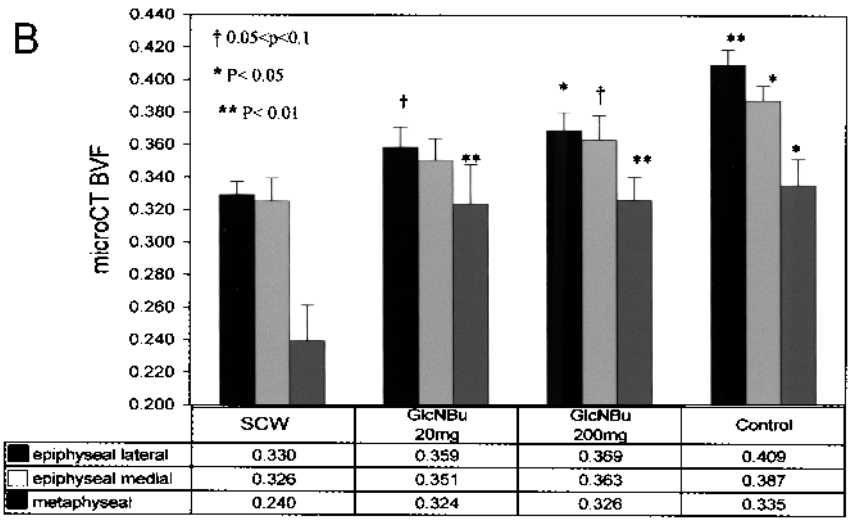

Figure 4. A. Bone mineral density (BMD) measured by DEXA. *Significant differences versus the SCW induced group. B. Bone volume fraction measured by micro-CT represents the fraction of voxels occupied by bone. *Significant differences versus the SCW induced group.

Table 1. Bone architecture changes analyzed by micro-CT.

Bone Measures	Regions of Interest	Treatments SCW	GlcNBu 20 mg	GlcNBu 200 mg	Control
3-D-BV/TV (%)	Lateral epiphysis	32.9 ± 0.8	35.9 ± 1.2*	37.0 ± 1.1*	42.2 ± 1.2**
	Medial epiphysis	32.3 ± 1.4	34.9 ± 1.3	36.0 ± 1.5*	40.5 ± 1.2*
	Metaphysis	23.9 ± 2.2	32.3 ± 2.5**	32.5 ± 2.5**	36.5 ± 1.5**
3-D-Tb.Th (μm)	Lateral epiphysis	60.0 ± 1.2	61.9 ± 2.1	62.5 ± 2.2	78.8 ± 1.3**
	Medial epiphysis	67.5 ± 1.5	70.0 ± 3.1	71.2 ± 3.4	90.2 ± 1.4**
	Metaphysis	34.5 ± 1.1	41.3 ± 1.6**	39.9 ± 1.3**	44.8 ± 1.2**
3-D-Tb.N (n/mm^3)	Lateral epiphysis	5.5 ± 0.11	5.82 ± 0.15	5.96 ± 0.18*	6.19 ± 0.24*
	Medial epiphysis	4.77 ± 0.13	5.02 ± 0.12	5.11 ± 0.20	5.27 ± 0.16
	Metaphysis	6.83 ± 0.53	7.73 ± 0.38	8.23 ± 0.44*	9.23 ± 0.32*
3-D-Tb.Sp (μm)	Lateral epiphysis	1.23 ± 0.03	1.11 ± 0.04*	1.07 ± 0.04**	1.04 ± 0.07**
	Lateral epiphysis	1.44 ± 0.07	1.30 ± 0.04	1.27 ± 0.06*	1.14 ± 0.08*
	Medial epiphysis	1.23 ± 0.14	0.91 ± 0.07*	0.85 ± 0.06*	0.74 ± 0.12**

* $p < 0.05$, ** $p < 0.01$ indicate significance compared to SCW group. SCW: streptococcal cell wall; BV: bone volume; TV: tissue volume; Tb.Th: trabecular bone thickness; Tb.N: trabecular number; Tb.Sp: trabecular separation; GlcNBu: N-butyryl glucosamine.

Table 2. Bone connectivity measures from the anterior, middle, and lateral sections of proximal tibia using micro-CT images.

Connectivity Measures	Group	Anterior Section Lateral	Anterior Section Medial	Middle Section Lateral	Middle Section Medial	Posterior Section Lateral	Posterior Section Medial
Endpoints	SCW	40.5 ± 5.6*	30.0 ± 4.1	21.9 ± 2.6*	15.8 ± 2.2*	21.4 ± 1.7*	20.8 ± 1.9*
	20 mg/kg/day	36.2 ± 2.5	22.5 ± 1.7	17.5 ± 1.9	14.1 ± 2.3	20.0 ± 1.8	16.2 ± 2.1
	200 mg/kg/day	34.1 ± 4.1	26.7 ± 5.7	19.8 ± 1.7	12.2 ± 2.1	16.3 ± 1.2	17.1 ± 1.8
	Control	15.5 ± 6.2	13.4 ± 3.8	10.3 ± 2.5	5.0 ± 1.1	10.0 ± 1.3	5.1 ± 1.5
Multiple points	SCW	7.5 ± 1.1*	8.5 ± 1.2*	6.8 ± 1.3	9.0 ± 1.0	7.1 ± 0.7*	13.7 ± 0.8*
	20 mg/kg/day	9.3 ± 1.6	9.2 ± 1.0	8.3 ± 1.1	9.9 ± 1.1	7.8 ± 0.8	12.6 ± 1.4
	200 mg/kg/day	10.3 ± 2.7	10.7 ± 1.7	9.5 ± 1.9	12.6 ± 1.8	9.8 ± 0.7	13.9 ± 1.8
	Control	16.4 ± 4.5	15.8 ± 1.3	9.8 ± 0.2	11.3 ± 0.3	17.4 ± 2.2	19.7 ± 8.5
Node-node struts	SCW	0.7 ± 0.2*	0.9 ± 0.2*	0.7 ± 0.2	1.2 ± 0.2*	0.7 ± 0.1*	1.5 ± 0.1*
	20 mg/kg/day	0.8 ± 0.2	1.2 ± 0.2	1.0 ± 0.2	1.2 ± 0.2	0.9 ± 0.1	1.7 ± 0.3
	200 mg/kg/day	1.2 ± 0.4	1.3 ± 0.3	0.9 ± 0.2	2.0 ± 0.3†	1.3 ± 0.2†	2.1 ± 0.3
	Control	3.3 ± 0.4	2.3 ± 0.6	1.0 ± 0.1	2.1 ± 0.0	1.3 ± 0.4	2.7 ± 0.8
Total strut length	SCW	4.9 ± 0.2*	4.8 ± 0.2	3.8 ± 0.2	4.3 ± 0.2	4.0 ± 0.2*	5.5 ± 0.2
	20 mg/kg/day	5.3 ± 0.4	5.1 ± 0.3	4.0 ± 0.2	4.2 ± 0.3	4.3 ± 0.2	5.7 ± 0.3
	200 mg/kg/day	5.4 ± 0.7	5.1 ± 0.5	4.2 ± 0.2	4.9 ± 0.3	4.8 ± 0.2†	5.6 ± 0.3
	Control	7.5 ± 0.9	5.9 ± 0.7	4.6 ± 0.3	4.7 ± 0.3	4.8 ± 0.1	6.3 ± 1.0

* $p < 0.05$ indicate significance versus control group. † $p < 0.05$ indicate significance versus SCW group. CT: computerized tomography; SCW: streptococcal cell wall.

induced group versus controls indicates elevated bone resorption in the arthritic joints. However, both 20 and 200 mg GlcNBu treatment showed significant beneficial effects in a dose-dependent manner (Figure 5).

Joint surface integrity. Isosurfaces generated from micro-CT scans of diseased bone showed clear bone erosion at the joint margin (Figure 6). However, protection against bone erosions was observed in the GlcNBu-treated groups, especially in the high-dose group. Figure 6 shows treated rat isosurfaces of the chondyles of proximal rat tibia in (a) SCW induced rat; (b) 20 mg GlcNBu-treated rat; (c) 200 mg GlcNBu-treated rat; and (d) control rat. Qualitative comparisons of the isosurfaces in these groups show that GlcNBu protects bone from erosion in this model of chronic inflammatory arthritis.

DISCUSSION

We found that oral administration of GlcNBu, administered at 2 doses, resulted in disease modification in an SCW induced arthritis rat model. There was significant improvement in direct measurement of joint inflammation, BMD, and bone microarchitecture with administration of GlcNBu. The protection afforded by GlcNBu is considerable. For the inflammatory measurements and most bone measures, the effect is maximal at the relatively high single oral dose (200 mg/kg/day), but for other measures the maximal effect is seen at the relatively low single oral dose (20 mg/kg/day). Our pharmacokinetic studies in the rat[28] indicate that similar orally administered doses of GlcNBu (233 mg/kg) resulted in concentrations in the venous circulation that rise early and decline slowly.

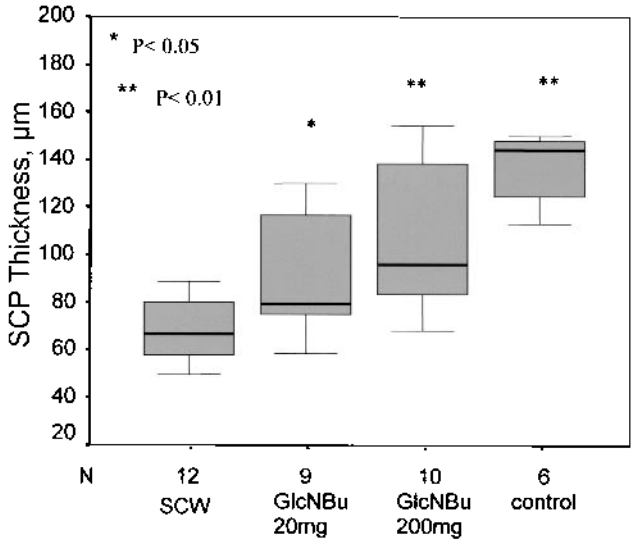

Figure 5. Subchondral plate (SCP) thickness measured from the central coronal section of proximal tibia from micro-CT images. *Significant differences versus the SCW induced group.

In the SCW arthritis model, bone loss and marginal bone destruction are the common form of bone change[37,38]. Several studies have described the pathological and structural changes in human arthritic joints[39-41]. However, the trabecular bone connectivity alterations and site-specific microarchitecture changes in inflammatory models have not been previously reported. Specifically, we report for the first time that trabecular connectivity is significantly decreased in the arthritic bone, and this decreased connectivity is considerably reversed or prevented by GlcNBu treatment. Another unique finding is the 3-D site-specific microarchitecture changes. It is important to note that the posterior part of the joint shows higher bone mass but not necessarily higher connectivity than the middle or anterior parts. Similarly, the medial side of a coronal section has higher bone volume and thickness, but no differences in connectivity compared to the lateral side. The SCW-mediated arthritis group also demonstrated site-specific changes; namely, the anterior part (particularly in the lateral side) showed more arthritic changes compared to other sites.

Distinct evidence for disease modifying activity for the

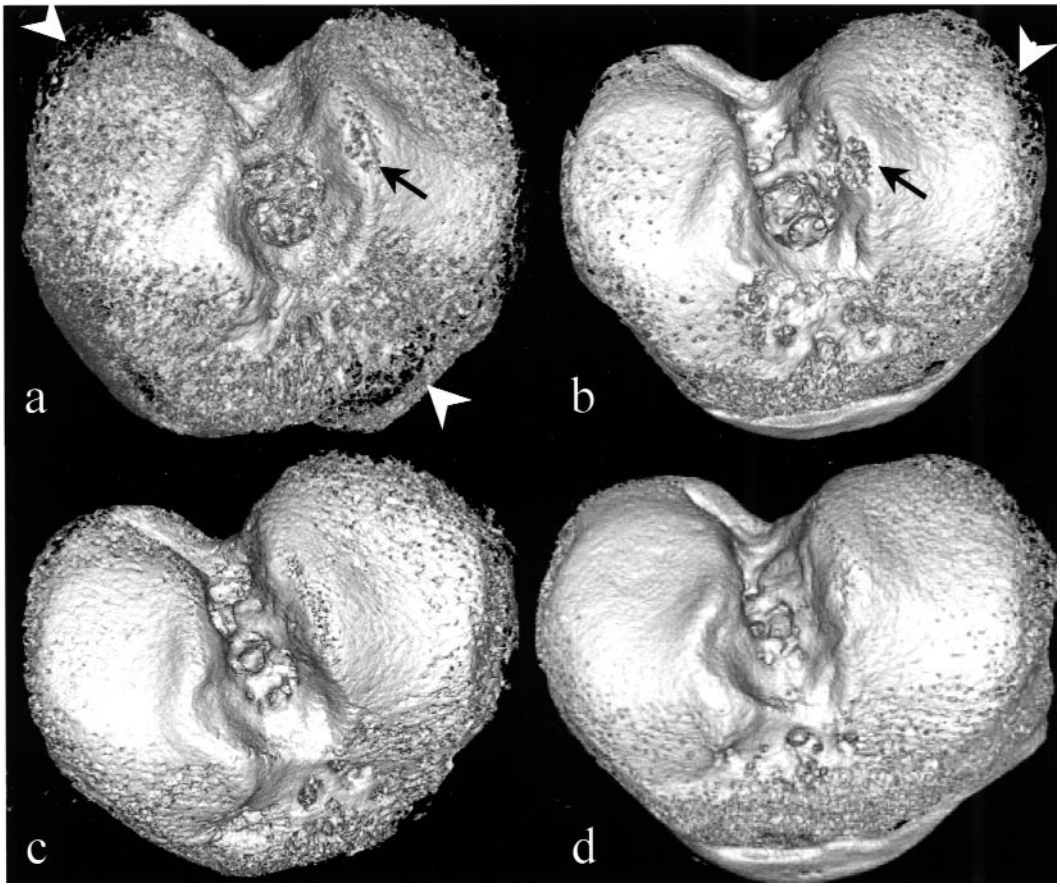

Figure 6. Segmented volume rendering of proximal tibia plateau shows different degree of bone erosion on the edge (white arrow) and on the top of the tibial plateau (black arrow) in various groups. Severe subchondral bone erosions were evident at the panus-bone interfaces of the epiphysis in the SCW induced arthritis (A). Treatment with 20 mg GlcNBu reduced bone loss in both sites (B). These erosions were diminished even more in rats treated with 200 mg GlcNBu (C). A smooth, intact surface is shown in control rat tibia (D).

compound was provided by the improvement observed in the micro-CT images, in which the arthritic joints were significantly protected by treatment at the 200 mg/kg/day dose and partially protected by treatment at the 20 mg/kg/day dose (Table 2). In addition, micro-CT technology, which is uniquely suited for comprehensive 3-D analysis of bony joint surface integrity (Figure 6) changes in the SCW induced arthritis rat model, showed clear protection with GlcNBu at both high and low doses. Connectivity evaluation showed that GlcNBu treatment resulted in protection of the subchondral cancellous bone connectivity and architecture. Improvement in bone density by DEXA was shown to be particularly significant in the distal tibia. Similar bone density protective effects have also been observed by treatment with cytokine inhibitors in a model of adjuvant induced arthritis in the rat[42].

Our findings demonstrate the bone-protective efficacy of GlcNBu in the Lewis rat model of SCW chronic destructive arthritis. It is not clear if the preventive changes in bone degradation are a result of the apparent antiinflammatory effect and decreased synovitis or if there is an independent effect on bone. The antiinflammatory effect can be modified somewhat by different feeding protocols, such as adding the same total daily dose to crushed chow, so that the lower amounts are consumed continually (unpublished data). Since the destructive phase does not develop until after 2 weeks in the SCW inflammatory arthritis (coincident with the increases in ankle size, Figure 3), it appears to make some sense, in terms of an RA model, to treat when the inflammation first appears, but before bone and cartilage destruction has commenced. This strategy would be particularly desirable if the administered compound has very low toxicity, as appears to be the case with GlcNBu.

A possible avenue of future investigation of the antiinflammatory effects of GlcNBu is through a glycobiology perspective. Synthetic fibronectin peptides are known to suppress SCW induced arthritis by interfering with leukocyte cell adhesion[43]. A large molecular weight hyperglycosylated fibronectin isoform, as well as a relatively underglycosylated isoform, are induced by treatment of bovine chondrocytes by TGF-ß1[44]. As indicated in the introduction, anti-TGF-ß antibodies reverse the SCW induced arthritis[31]. Preliminary work from one of our research groups (TA) indicates that the hyperglycosylated fibronectin isoform does not bind antibodies such as rheumatoid factor, which are readily bound by the lower molecular weight underglycosylated isoform, and that glycosylation of fibronectin may be affected by the addition of GlcNBu in some cell culture systems. A variety of antibodies have been identified in SCW induced arthritis[45]; thus, antibody binding to hyperglycosylated and underglycosylated fibronectin in animals treated and not treated with GlcNBu could provide some insight into a mechanism of action for the antiinflammatory effects of this compound.

In addition, it is possible that the preventive effect of GlcNBu on bone degradation in this model was mediated through directly inhibited osteoclast numbers and function or by increasing the number of osteoblasts at sites of bone erosion. Comparison of the isosurfaces and the architectural measures showed that GlcNBu effectively protected bone from further erosion in this model. However, the metaphyseal bone structure changes suggest that GlcNBu functions systemically.

Taken together, our findings indicate that GlcNBu has the potential for development either as a stand-alone treatment for inflammatory joint diseases with bone loss or in combination with other antiinflammatory and/or bone growth-promoting agents. The findings also suggest that evaluation of GlcNBu in a noninflammatory animal model with bone loss, such as the ovariectomized rat, might reveal whether the effects observed were dependent on suppression of the inflammatory response or whether this drug affects bone metabolism directly. Work with the ovariectomized rat model currently in progress includes a control group where GlcNBu is fed to normal animals, in order to assess the potential for prevention strategies.

REFERENCES

1. Bogoch ER, Moran E. Abnormal bone remodelling in inflammatory arthritis. Can J Surg 1998;41:264-71.
2. Duncan H. Cellular mechanisms of bone damage and repair in the arthritic joint. J Rheumatol Suppl 1983;11:29-37.
3. Sokoloff L. Osteoarthritis as a remodeling process. J Rheumatol 1987;14 Spec No:7-10.
4. Goldring SR. Bone and joint destruction in rheumatoid arthritis: what is really happening? J Rheumatol 2002;29 Suppl 65:44-8.
5. Anastassiades T, Rees-Milton K. Biochemical markers for osteoarthritis: from the present to the future and back to the past [editorial]. J Rheumatol 2005;32:578-9.
6. Tchetina EV, Squires G, Poole AR. Increased type II collagen degradation and very early focal cartilage degeneration is associated with upregulation of chondrocyte differentiation related genes in early human articular cartilage lesions. J Rheumatol 2005;32:876-86.
7. Hooyman JR, Melton LJ III, Nelson AM, O'Fallon WM, Riggs BL. Fractures after rheumatoid arthritis. A population-based study. Arthritis Rheum 1984;27:1353-61.
8. Spector TD, Hall GM, McCloskey EV, Kanis JA. Risk of vertebral fracture in women with rheumatoid arthritis. BMJ 1993;306:558.
9. Fuchs HA, Kaye JJ, Callahan LF, Nance EP, Pincus T. Evidence of significant radiographic damage in rheumatoid arthritis within the first 2 years of disease. J Rheumatol 1989;16:585-91.
10. McGonagle D, Conaghan PG, O'Connor P, et al. The relationship between synovitis and bone changes in early untreated rheumatoid arthritis: a controlled magnetic resonance imaging study. Arthritis Rheum 1999;42:1706-11.
11. Klarlund M, Ostergaard M, Rostrup E, Skjodt H, Lorenzen I. Dynamic magnetic resonance imaging of the metacarpophalangeal joints in rheumatoid arthritis, early unclassified polyarthritis, and healthy controls. Scand J Rheumatol 2000;29:108-15.
12. Goldring SR. Pathogenesis of bone and cartilage destruction in rheumatoid arthritis. Rheumatology Oxford 2003;42 Suppl 2:ii11-ii16.
13. Wyllie JC. Histopathology of the subchondral bone lesion in rheumatoid arthritis. J Rheumatol Suppl 1983;11:26-8.
14. Scott DL, Pugner K, Kaarela K, et al. The links between joint damage and disability in rheumatoid arthritis. Rheumatology Oxford 2000;39:122-32.

15. Pincus T. Rheumatoid arthritis: disappointing long-term outcomes despite successful short-term clinical trials. J Clin Epidemiol 1988;41:1037-41.
16. Welsing PM, van Gestel AM, Swinkels HL, Kiemeney LA, van Riel PL. The relationship between disease activity, joint destruction, and functional capacity over the course of rheumatoid arthritis. Arthritis Rheum 2001;44:2009-17.
17. Sharp JT, Lidsky MD, Collins LC, Moreland J. Methods of scoring the progression of radiologic changes in rheumatoid arthritis. Correlation of radiologic, clinical and laboratory abnormalities. Arthritis Rheum 1971;14:706-20.
18. Genant HK, Jiang Y, Peterfy C, Lu Y, Redei J, Countryman PJ. Assessment of rheumatoid arthritis using a modified scoring method on digitized and original radiographs. Arthritis Rheum 1998;41:1583-90.
19. Chan E, Pandith V, Towheed TE, Brouillard D, Zee B, Anastassiades TP. Comparison of the combined cortical thickness of the second metacarpal with Sharp's method for scoring hand microradiographs in rheumatoid arthritis. J Rheumatol 1998;25:1290-4.
20. Yu W, Xie YZ, Jiang M, et al. CT detection of wrist bone erosion in rheumatoid arthritis. Chin Med J Engl 1993;106:509-13.
21. Choy EH, Smith C, Dore CJ, Scott DL. A meta-analysis of the efficacy and toxicity of combining disease-modifying anti-rheumatic drugs in rheumatoid arthritis based on patient withdrawal. Rheumatology Oxford 2005;44:1414-21.
22. Towheed TE, Anastassiades TP, Shea B, Houpt J, Welch V, Hochberg MC. Glucosamine therapy for treating osteoarthritis. Cochrane Database Syst Rev 2001;1:CD002946.
23. Cibere J, Kopec JA, Thorne A, et al. Randomized, double-blind, placebo-controlled glucosamine discontinuation trial in knee osteoarthritis. Arthritis Rheum 2004;51:738-45.
24. Development of N-acylated glucosamines (GlcNAcyls) for arthritic conditions. 5th ICRS Symposium, Ghent, Belgium: 2004.
25. Terry DE, Rees-Milton K, Smith P, et al. N-acylation of glucosamine modulates chondrocyte growth, proteoglycan synthesis, and gene expression. J Rheumatol 2005;32:1775-86.
26. Poustie MW, Carran J, McEleney K, Dixon SJ, Anastassiades TP, Bernier SM. N-butyryl glucosamine increases matrix gene expression by chondrocytes. J Pharmacol Exp Ther 2004;311:610-6.
27. Brockhausen I, Carran J, McEleney K, et al. N-Acyl derivatives of glucosamine as acceptor substrates for galactosyltransferase from bone and cartilage cells.Carbohydr Res 2005;340:1997-2003.
28. Aghazadeh-Habashi A, Carran J, Anastassiades T, Jamali F. High performance liquid chromatographic determination of N-butyryl glucosamine in rat plasma. J Chromatogr B Analyt Technol Biomed Life Sci 2005;819:91-6.
29. Tiraloche G, Girard C, Chouinard L, et al. Effect of oral glucosamine on cartilage degradation in a rabbit model of osteoarthritis. Arthritis Rheum 2005;52:1118-28.
30. Xxxxx. CRC Handbook of Animal Models for the Rheumatic Diseases. Ref Type: Serial (Book,Monograph). CRC Press Inc., 1988.
31. Wahl SM, Allen JB, Costa GL, Wong HL, Dasch JR. Reversal of acute and chronic synovial inflammation by anti-transforming growth factor beta. J Exp Med 1993;177:225-30.
32. Kimpel D, Dayton T, Fuseler J, et al. Splenectomy attenuates streptococcal cell wall-induced arthritis and alters leukocyte activation. Arthritis Rheum 2003;48:3557-67.
33. Nagy TR, Prince CW, Li J. Validation of peripheral dual-energy X-ray absorptiometry for the measurement of bone mineral in intact and excised long bones of rats. J Bone Miner Res 2001;16:1682-7.
34. Feldkamp LA, Goldstein SA, Parfitt AM, Jesion G, Kleerekoper M. The direct examination of three-dimensional bone architecture in vitro by computed tomography. J Bone Miner Res 1989;4:3-11.
35. Hildebrand T, Laib A, Muller R, Dequeker J, Ruegsegger P. Direct three-dimensional morphometric analysis of human cancellous bone: microstructural data from spine, femur, iliac crest, and calcaneus. J Bone Miner Res 1999;14:1167-74.
36. Parisien M, Mellish RW, Silverberg SJ, et al. Maintenance of cancellous bone connectivity in primary hyperparathyroidism: trabecular strut analysis. J Bone Miner Res 1992;7:913-9.
37. Chan JM, Villarreal G, Jin WW, Stepan T, Burstein H, Wahl SM. Intraarticular gene transfer of TNFR:Fc suppresses experimental arthritis with reduced systemic distribution of the gene product. Mol Ther 2002;6:727-36.
38. Funk JL, Chen J, Downey KJ, Davee SM, Stafford G. Blockade of parathyroid hormone-related protein prevents joint destruction and granuloma formation in streptococcal cell wall-induced arthritis. Arthritis Rheum 2003;48:1721-31.
39. Barrie HJ. Pathology of femoral heads in patients with rheumatoid disease. J Rheumatol 1990;17:448-59.
40. Eulderink F, Meijers KA. Pathology of the cervical spine in rheumatoid arthritis: a controlled study of 44 spines. J Pathol 1976;120:91-108.
41. Bruser P. Pathology of the sesamoid bones of the hand [German]. Handchir Mikrochir Plast Chir 1994;26:302-6.
42. Badger AM, Griswold DE, Kapadia R, et al. Disease-modifying activity of SB 242235, a selective inhibitor of p38 mitogen-activated protein kinase, in rat adjuvant-induced arthritis. Arthritis Rheum 2000;43:175-83.
43. Wahl SM, Allen JB, Hines KL, et al. Synthetic fibronectin peptides suppress arthritis in rats by interrupting leukocyte adhesion and recruitment. J Clin Invest 1994;94:655-62.
44. Rees-Milton KJ, Terry D, Anastassiades TP. Hyperglycosylation of fibronectin by TGF-beta 1-stimulated chondrocytes. Biochem Biophys Res Commun 2004;317:844-50.
45. Nesher G, Moore TL, Grisanti MW, el Najdawi E, Osborn TG. Correlation of antiperinuclear factor with antibodies to streptococcal cell-wall peptidoglycan-polysaccharide polymers and rheumatoid factor. Clin Exp Rheumatol 1991;9:611-5.